JOURNAL OF ECONOMICS AND ADMINISTRATIVE SCIENCES

E-ISSN: 2227-703X P-ISSN: 2518-5764

Volume 32 | Number 2 57 - 70

6-30-2026

Nonparametric Control Charts Estimation Using Hybrid Cyber-Intelligence Algorithms for Stock Market Monitoring

Mariam Jumaah Mousa
Department Banking and Financial, Imam Alkadhim University College, Baghdad, Iraq, maram.alamy@iku.edu.iq

Munaf Yousif Hmood
Department of Statistics, College of Administration and Economics, University of Baghdad, Baghdad, Iraq, munaf.yousif@coadec.uobaghdad.edu.iq

JOURNAL OF ECONOMICS AND ADMINISTRATIVE SCIENCES 2026;32(2):57–70

RESEARCH ARTICLE

Nonparametric Control Charts Estimation Using Hybrid Cyber-Intelligence Algorithms for Stock Market Monitoring

Mariam Jumaah Mousa [a,*], Munaf Yousif Hmood [b]

[a] Department Banking and Financial, Imam Alkadhim University College, Baghdad, Iraq
[b] Department of Statistics, College of Administration and Economics, University of Baghdad, Baghdad, Iraq

Abstract

This paper introduces a novel nonparametric hybrid cyber-intelligence-based statistical process control and anomaly detection framework in time series data. It is developed to overcome the shortcomings of the classical control schemes in dealing with complex, abnormal, and noisy input data, especially when it is autocorrelated. The proposed methodology combines three technical pillars: First, it utilizes a bidirectional long-short-term memory architecture (Bi-LSTM) to capture long-term time dependency and learn nonlinear patterns, leaving only true deviations as residuals that remove trends and noises from the market. Second, it adopts the Golden Eagle Optimizer (GEO) algorithm for optimal parameter selection. This intelligent algorithm tunes the smoother factor (l) and the control boundary (L) at a certain sample size to minimize the Average Run Length (ARL) of the nonparametric exponentially weighted moving average (NPEWMA-SR) scheme. Third, the framework is validated via R software. The framework was applied to Google's daily trading data using different sample sizes (10, 30, 60, 120, 250, 365, 600, 900, and 1245) days of 2026, to detect the shift in the system, within 2 trading days, achieving an In-control Average Run Length ARL0 = 499.6 and an Out-of-control Average Run Length ARL1 = 1.65 days. The system demonstrated high statistical stability, a very low false alarm rate, and the best statistical sensitivity among all sample sizes. These results prove its effectiveness across small, medium, and large samples, making it a powerful early warning system for monitoring market volatility.

Keywords: Nonparametric control charts (NPEWMA-SR), Bidirectional long short-term memory (Bi-LSTM), Golden eagle optimizer (GEO), Time series anomaly detection, Google stock returns monitoring

1. Introduction

Precise prediction and tracking of time series data remains a central challenge of statistical process control, particularly in the case of complex data exhibiting high volatility and non-normal distributions. Traditional parametric control charts such as Shewhart and exponentially weighted moving average (EWMA) charts assume that the underlying data is normally distributed. In contemporary industrial and financial problems, data often violates this assumption, and may be skewed in distribution or have heavy tails. Therefore, traditional charts produce elevated false alarm rates or fail to detect actual structural changes in a timely fashion. In order to overcome such constraints, there is an urgent need to adopt advanced artificial intelligence to improve monitoring efficiency. The initial application of machine learning in this research is a Bidirectional Long Short-Term Memory architecture with an Attention Mechanism. The model uniquely captures complicated temporal relationships and nonlinear relationships which the conventional methods do not consider and thus it can generate accurate residuals, which identify true signals and exclude underlying noise and global trends. After the modeling and extraction of the residues, the need for Nonparametric Control Charts emerges since they do not assume any

Received 19 April 2026; revised 10 June 2026; accepted 13 June 2026.
Available online 30 June 2026

* Corresponding author.
E-mail addresses: maram.alamy@iku.edu.iq (M. J. Mousa), munaf.yousif@coadec.uobaghdad.edu.iq (M. Y. Hmood).

https://doi.org/10.33095/2227-703X.4350

distribution. One of the most resilient tools in this context is the Nonparametric Exponentially Weighted Moving Average Signed-Rank (NPEWMA-SR) chart: because it is based on data ranks and not the data values themselves, it does not allow random outliers to continue to affect the residuals. The scientific power of this combination is that the Bidirectional Long Short-Term Memory model can study the dynamics of the series, and the nonparametric chart guarantees stable monitoring under unknown distributions. Although this chart is robust, the smoothing factor (λ) and the control limit coefficient (L) for both are important to determine its efficiency. Thus, this paper uses nature-inspired intelligence through the Golden Eagle Optimizer (GEO) to tune these parameters dynamically and adaptively with respect to the size of the sample and volatility. The objective of this sequence is to develop a hybrid surveillance system that is both deep-learning-precise and nonparametric statistical-robustness such that a low Average Run Length (ARL_1) is minimized during shifts and rapid response to process anomalies. The methodology is used to prove the practical effectiveness of this framework, using Google stock returns with several samples. This research article is organized as follows: Section 2 gives an overview of the literature on statistical monitoring and control schemes. Section 3 examines the methodology employed, including a long-term bidirectional memory model, the Golden Eagle optimizer and the NPEWMA-SR. Section 4 presents the applied results and discusses the performance of the hybrid model on the sample size using Google Stocks data. Lastly, Section 5 wraps up the paper by summarizing the key findings.

2. Literature review and hypothesis development

The history of Statistical Process Control (SPC) has changed dramatically to nonparametric approaches owing to their intrinsic flexibility and immunity to distributional biasness. Graham et al. (2011) introduced a pioneering research on the nonparametric exponentially weighted signed rank chart (NPEWMA-SR) and showed that the combination of Wilcoxon signed-rank statistics and the EWMA mechanism offers practical recommendations on setting design parameters with the only important point to note that the smoothing coefficient λ must be as small as possible (0.0502) to capture small variations, whereas the limit coefficient (L) was set to a desired ARL_0. Expanding on this, the NPEWMA-SN chart was used by da Cruz et al. (2019) to track the water quality (Chemical Oxygen Demand). Their approach was to achieve the goal by choosing λ to capture the historical data and to modify L to achieve statistical stability in non-normal environment data, where they find that this methodology helps avoid high false alarm rates common to parametric charts.

In 2020, sampling efficiency and industrial applications were investigated (Ali et al., 2020) created an NPREWMA-SN chart under a Ranked Set Sampling (RSS) scheme. Applying Monte Carlo simulations to calculate optimum (λ, L) values they established that this scheme has a high sensitivity to small-to-medium shifts compared to simple random sampling. At the same time Rahman et al. (2023) showed that the nonparametric panels are practically robust in the food sector and that they could be used to track the fat content of animal feed in unknown distributions. The research took a new direction and focused on specialized detection and sensitivity improvement. Bogo et al. (2023) applied them in the water resources sector to identify the presence of leaks in residential complexes, and Talordphop et al. (2023) suggested the extended version (EEWMA-SR), which was found to be more effective in detecting very small shifts than its predecessors.

In 2024, advanced modeling came into the limelight. Azadeh et al. (2024) used deep learning to predict panel features and address measurement error ties. In the meantime, Raza et al. (2024) used these charts in the monitoring of networks with regard to cybersecurity. In particular, Raza et al. (2024) put forward a hybrid NPEWMA-MA chart of gas turbines, whereby a formula of a corrected variance is employed in improving the control limits. They optimized L and (λ) in their study to provide dynamic weights to the recent data, and they were better than the traditional nonparametric charts in different distributions.

The latest developments in 2025 and 2026 are aimed at multi-dimensional data structures and smart optimization. Kumar et al. (2025) combined blockchain with intelligent algorithms to ensure reliability of financial signals, and Herdiani et al. (2025) proceeded to validate these methods in the food sector, (Phantu et al., 2025) handled the issue of Zero-Inflated Data by coming up with a modified EWMA chart that is based on sign ranks. Their methodology maximized the smoothing factor to enhance sensitivity to shifts in the probability of small-scale inflation, giving excellent protection against false alarm in count data. As suggested by Cui et al. (2025) triple generally weighted moving average (TGWMA) sign chart is proposed in this study for monitoring the process when the underlying distribution is unknown. on the other hand, Nor Fashihah (2025) presented robust memory-type control panels for monitoring site features under abnormal data conditions with skewed distributions

Table 1. Comparison of the proposed framework with key literature.

Study	Method	Application	Key Finding	Limitation
Graham et al. (2011)	NPEWMA-SR	General	Foundation of signed-rank charts	Fixed parameters
Talordphop et al. (2023)	EEWMA-SR	Process monitoring	Better for small shifts	No optimization
Raza et al. (2024)	NPEWMA-MA	Gas turbines	Dynamic weights	No deep learning
This study	Bi-LSTM+GEO+NPEWMA-SR	Financial returns	$ARL_1 = 1.65$	Single asset

and heavy tails. Lastly Sudsutad et al. (2026) concentrated on hybrid EWMA and Double Moving Average methods of symmetric and non-symmetric distributions, and Ding et al. (2026) proved that these two robust principles were accurate in medical image segmentation. This successive development serves to emphasize the fact that NPEWMA-SR framework and its variations have turned into an invaluable asset in numerous fields because of their great flexibility and consistency in statistical results.

However, to the best of our knowledge, no prior study has combined the Bi-LSTM network with the Golden Eagle Optimizer (GEO) for NPEWMA-SR control chart optimization, which defines the core motivation and gap addressed by this research.

Then, based on this literature review, the following hypotheses were formulated for our current research:

Hypothesis 1: The proposed hybrid model achieves a statistically significant reduction in ARL_1 values for detecting small and medium-sized deviations compared to traditional NPEWMA-SR charts.

Hypothesis 2: The Golden Eagle Optimizer (GEO) identifies optimal parameter pairs (λ, L) that outperform fixed parameter tables in reducing false alarm rates

Hypothesis 3: The integration of the attention mechanism with Bi-LSTM improves early detection of process deviations compared to Bi-LSTM without attention.

Hypothesis 4: The hybrid Bi-LSTM-GEO model maintains ARL_0 near target (500) across sample sizes n = 10 to n = 1,254, demonstrating statistical robustness.

To provide a clear overview of the existing literature and emphasize the unique contribution of this research, Table 1 summarizes and compares the key related studies with the proposed framework.

3. Methodology

This section reviews a proposed framework that integrates deep learning techniques and nature-inspired algorithms with nonparametric qualitative control panels. The proposed design aims to enhance the accuracy of detecting small shifts in processes that do not follow a normal distribution.

3.1. Nonparametric exponentially weighted moving average signed-rank chart (NPEWMA-SR)

The NPEWMA-SR (Nonparametric Exponentially Weighted Moving Average Signed-Rank) panel is defined as a sophisticated nonparametric statistical control tool designed to monitor the position parameter (median) in processes that do not necessarily follow a normal distribution. Its construction is based on combining the robust Wilcoxon Signed-Rank statistical power characterized by its resilience against outliers with the Exponentially Weighted Moving Average (EWMA) mechanism, which gives the panel exceptional sensitivity to detecting small deviations in the process (Graham et al., 2011). Its core function is to transform raw data into signed ranks relative to the target value, making it a "distribution-free" panel; its control performance is unaffected by the original data distribution as long as it remains symmetrical (Talordphop et al., 2023).

The NPEWMA-SR chart is constructed by accumulating statistics sequentially from each subgroup. The plotting statistic is:

$$Z_i = \lambda \, SN_i + (1-\lambda)\, Z_{i-1} \qquad for\ i = 1, 2, 3, \ldots, \quad \ldots \quad (1)$$

Where:

λ Smoothing parameter, that determines the speed of the panel's response; its value ranges from $0 < \lambda \leq 1$. Smaller values make the panel faster at detecting minor shifts (Talordphop et al., 2023).

SN_i Signed rank statistics, which represents the value extracted from the current sample after converting the observations into ranks.

It is calculated for each t time sample of size n, using the following formula (Herdiani et al., 2025; Rahman et al., 2023), $SN_i = Sign\left(x_{ij} - \theta_0\right) R_{ij}$

R_{ij} denote the rank of the absolute values of the differences,

$|x_{ij} - \theta_0|$, The sign function that gives (+1) for positive differences and (–1) for negative differences, θ_0 is the known or the specified or the target value of the media.

Z_{i-1} The value of the previous board represents the cumulative information learned from previous samples, and usually begins with $Z_0 = 0$.

To achieve the control chart goal of monitoring process quality over time, it consists of three main lines: the first center line (CL = 0) and the second upper control limit (UCL), and the lower control limit (LCL) as:

$$ULC = L\sqrt{\frac{n\,(n+1)\,(2n+1)}{6}\left(\frac{\lambda}{2-\lambda}\right)},$$
$$LCL = -L\sqrt{\frac{n\,(n+1)\,(2n+1)}{6}\left(\frac{\lambda}{2-\lambda}\right)} \tag{2}$$

L is a parameter that defines the boundary width for controlling the false alarm rate. The term $\frac{n(n+1)(2n+1)}{6}$ represents the variance of the Wilcoxon signed-rank statistic SN_i (Talordphop et al., 2023)

3.2. Run-length distribution

The run-length (RL) defined in Chakraborti and Graham (2018) is a random variable that indicates the number of points (board statistics) that must be plotted (or the number of subsets that must be collected, each producing one board statistic) before the board gives its first out-of-control (OOC) signal (or before the first alert event is observed). This indicates the extent to which the panel is able to distinguish between the stable state (In-Control) and the state that suffers from shifts (Out-of-Control).In order to calculate the run length distribution and its associated properties, the Graham et al. (2011) using the Markov chain method, it is possible to find explicit expressions (mathematical formulas) for the properties of interest, given that the Markov chain representation of the run length distribution is in the case of an IC-controlled process, the probability mass function (pmf) and the expected value (ARL) and the cumulative distribution function (cdf) of the run-length variable N can all be calculated as:

$$P\,(N=t;\lambda,L,r,\theta) = \xi Q^{t-1}\,(I-Q)\,e \quad for\, t = 1,2,3,\ldots, \tag{3}$$

$$ARL\,(\lambda,L,r,\theta) \;=\; \xi(I-Q)^{-1}e \tag{4}$$

$$P\,(N\leq t;\lambda,L,r,\theta) = 1-\;\xi(Q)^{t}e \qquad for\, t = 1,2,3,\ldots, \tag{5}$$

where r + 1 denotes the total number of states (i.e. there are r non-absorbing states and one absorbing state which is entered when the chart signals),

$I = I_{r*r}$ is the identity matrix,

$Q = Q_{r*r}$ is called the essential transition probability sub-matrix which contains all the probabilities of going from one non-absorbing state to another,

$e = e_{r*1}$ is a column vector with all elements equal to one and

$\xi = \xi_{1*r}$ is a row vector called the initial probability vector which contains the probabilities that the Markov chain starts in a given state.

The vector $\xi = (\xi_{-m},\ldots,\xi = \xi_m)$ with m = (r–1)/2, is characteristically selected such that $\sum_{-m}^{m}\xi = 1$. We set $\xi_0 = 1$ and let $\xi_i = 0$ for all $i \neq 0$; this infers that $z_0 = 0$ with probability one, A key component in employing Markov chain approach is to get the essential transition probability sub-matrix Q_{r*r}. The components for the latter are termed as one-step transition probabilities; $Q_{r*r} = [p_{ij}]$ for i, j = –m, –m+1,...,m–1, m. The transition probability p_{ij} stands for conditional probability which a plotting statistic at time k, z_k, lies within state j, given that a plotting statistic at time k–1, z_{k-1}, lies within state i (an approximation to a latter probability is gotten through setting z_{k-1} equal to s_i that represents a midpoint of state i) and we get

$$p_{ij} = P(s_i-\gamma < z_k \leq s_i+\gamma\,|z_{k-1} = s_i) \tag{6}$$

The continuous range between LCL and UCL is divided into r = 2m + 1 equally spaced intervals of width γ = (UCL – LCL)/r. The midpoint of state j is s_j = LCL + (j + 0.5)γ for j = –m,. . . , m–1, m. The transition probability $p_{\{ij\}}$ is then approximated by evaluating the cumulative distribution function of the standardized chart statistic.

To evaluate the performance of the **NPEWMA-SR** chart, the Average Run Length (ARL) is employed as a key metric. While the Markov chain approach provides the theoretical framework for calculating the run-length distribution, the ARL values for the in-control (ARL_0) and out-of-control (ARL_1) states are determined based on the asymptotic normality of the test statistic as described by Graham et al. (2011).

The ARL_0 is used to establish the false alarm rate and is calculated as:

$$ARL_0 = \frac{1}{2\Phi\,(-L)} \tag{7}$$

For a specific shift δ in the process median, the ARL_1 is calculated to assess the chart's sensitivity:

$$ARL_1 = \frac{1}{\Phi\,(L.se_z-\delta)-\Phi\,(-L.se_z-\delta)} \tag{8}$$

where Φ denotes the standard normal cumulative distribution function and $se_z = \sqrt{\frac{\lambda}{2-\lambda}}$ (Graham et al., 2011; Talordphop et al., 2023).

Table 2. Structural specifications of the proposed standalone Bi-LSTM architecture.

Layer	Type	Units	Activation	Dropout
LSTM 1	Bidirectional	64	tanh	0.2
LSTM 2	Bidirectional	32	tanh	0.2
Dense	Fully connected	16	ReLU	0.1
Output	Dense	1	Linear	-

3.3. *Implementation of the chart*

3.3.1. *Deep temporal feature extraction*

This step is the cornerstone of the proposed model, employing a bidirectional long-short-term memory network (Bi-LSTM) in Kitaw Mekonen (2025) to process the raw data before converting it into signed ranks.

This process yields more stable values to represent the signed ranks (SN) and reduces the variance caused by randomness in the raw data, resulting in a more accurate string length distribution (RL) calculated in subsequent steps.

The Bi-LSTM acts as an intelligent filter, untangling complex correlations in the data as an integrated "intelligent preprocessor" within the Graham system. Instead of relying on fluctuating instantaneous values, the network uses its "gates" to control the flow of information: the forgetting gate, which removes noise that could trigger false alarms in the Graham control chart, and the input gate, which captures only intrinsic changes and stores them in the cell state.

Therefore, the input processing mechanism (x_t) within the Long-Term Memory (LTM) cell, upon input of the value x_t at time t, performs the following mathematical operations within the forward layer to process the data from t = 1 to T. The backward LSTM the same sequence chronologically in reverse order, from $T = t\,tot = 1$ as follows (Fri et al., 2025; Xie et al., 2024):

Forget Gate (f_t): Determines the amount of information to be retained from the past h_{t-1} based on the current input x_t:

$$f_t = \sigma\left(W_f.\,[h_{t-1}, x_t] + b_f\right) \tag{9}$$

1- Input Gate (i_t): Determines the new information that x_t will add to long-term memory.

$$i_t = \sigma\left(W_i.\,[h_{t-1}, x_t] + b_i\right) \tag{10}$$

2- Long Term Memory Update (c_t): Here, the history is combined with the present x_t to produce a revised memory state.

$$c_t = f_t * c_{t-1} + i_t * [\tanh\left(W_c.\ [h_{t-1}, x_t] + b_c\right) \tag{11}$$

3- The hidden aspect is the clever director who combines the present and the past.

$$h_t = \sigma\left(W_o.\,[h_{t-1}, x_t] + b_o\right) * \tanh\left(c_t\right) \tag{12}$$

Therefore, after implementing the mathematical formula Forward LSTM, we obtain $\overrightarrow{h_t}$ and Backward LSTM, we obtain $\overleftarrow{h_t}$, $H_t = [\overrightarrow{h_t}, \overleftarrow{h_t}]$

The final output of the first step (H_t) combines the memory outputs from both paths to produce the initialized value that will be entered into Graham's model. This is the primary input for the second step (optimization and rank formulation).

The hyperbolic tangent function is called tanh and the sigmoid activation function is σ. The parameters of W and b are trained.

The layout of the proposed standalone Bi-LSTM model with the number of layers, hidden units, and activation functions is specified in Table 2 to give a comprehensive view of the model structure and to tackle the lack of transparency in the network configuration.

To ensure architectural transparency and full reproducibility of the experimental design, the network was compiled and trained under a rigorous configuration framework.

The weight of the network connections were optimized by Adam with a standard learning rate set to 0.001, which is a suitable learning rate for stable convergence. In this case, the learning objective was controlled using the Mean Squared Error (MSE) loss function. There was a trade-off between processing speed and memory usage, so the time-series inputs were processed sequentially with a batch size of 32.

The training horizon was bounded by a maximum of 100 epochs, integrated with an Early Stopping mechanism featuring a patience parameter of 10 epochs to dynamically halt execution upon validation stall and mitigate overfitting.

Furthermore, the historical dataset of Google stock returns was partitioned sequentially into three non-overlapping subsets: a 70% training set to update the internal gated parameters, a 15% validation set to monitor training trajectories, and a 15% independent testing set dedicated to validating the final out-of-sample detection performance of the optimized Graham control scheme.

3.3.2. Choice of design parameters

The effectiveness of the NPEWMA-SR monitoring panel is highly reliant on the design parameters of the panel being carefully chosen: the smoothing coefficient (lambda) and the control limit width coefficient (L). These parameters are used to define the sensitivity and speed of the panel to detect deviations.

Selection of traditional design parameters (lambda, L) (in Graham et al., 2011) depends on the desired size of the shift lambda (Smoothing Parameter) Small values (0.05) are selected to detect small shifts, and large values (e.g., 0.20) are selected to detect large shifts. L (Control Limit Coefficient): This is established together with lambda to provide a given value of the mean string length under control (ARL_0) which is usually 370 or 500.

The study proposes an intelligent and automated solution as an alternative to using fixed tables or manual selection, as this may not be suitable for dynamic data. The conventional search is replaced with an "exhaustive optimization mechanism" which is guided by the Golden Eagle Optimizer (GEO) algorithm in order to find the best (lambda, L) combination for the most statistical efficient search.

This algorithm is proposed as a powerful nature-inspired metaheuristic optimization algorithm to mathematically model the complex hunting and flying motion and trajectory of the golden eagle. The main idea behind the optimizer is to balance between global exploration and local exploitation; the flight behavior is divided into two main operational phases: cruising and attacking. The golden eagle is a macro global searcher used for searching the multidimensional search space during the cruise phase, to identify promising coordinate zones. After the location of a possible prey is spotted and saved, the eagle enters attack mode and starts an intensive local exploitation phase, targeting the identified location. The algorithm relates to the mechanical process in two ways: It builds an orthogonal cruise hyper plane which is tangent to the eagle's position and is used to control the paths to explore the vectors while using a direct line of sight vector in the attack exploitation. This is an integrated kinematic update that allows the system to dynamically adapt the searching vectors to avoid early convergence and to guarantee high precision of the optimal control chart parameter configurations extracted (Amor et al., 2022; Mohammadi-Balani et al., 2021; Yu et al., 2025).

To completely combine the intelligence of Bi-LSTM with the decision made by Graham, a fitness function was developed to serve as a measure of the quality of the values the eagle hunts. The algorithm will minimize the following functions:

$$Minimize\ f(\lambda, L) = w_1.\left|ARL_{0,att} - ARL_{0,trg}\right| + w_2.ARL_1 \qquad (13)$$

$|ARL_{0,att} - ARL_{0,trg}|$ (Stability Criterion): This is the difference between the target value of the average length of the strings (e.g., 370) and that obtained with the selected parameters. This will be aimed at making this approach zero difference in order to make the panel reliable under controlled conditions.

ARL_1 (Sensitivity Criterion): A sensitivity criterion is a criterion that requires the panel to detect deviations at a certain speed. This value is obtained using refined features derived out of the Bi-LSTM layer so that the speed at which the detection is made depends on an in-depth perception of the data, rather than shallow reading.

w_1, w_1 The two are weighting coefficients which allow the researcher to adjust either for the stability of the panel (i.e., false alarms) or for the sensitivity of the panel (i.e., speed of error detection) according to practical applications.

Although Markov chains seem to be a theoretical approach, the hybrid nature of the system combining artificial intelligence (Bi-LSTM) and natural optimisation (GEO) algorithms demands computational flexibility and swift response time. Thus, in this study, Continuous Integral Approximation was used as an effective and reliable alternative. This approach is based on the "Asymptotic Normality" of the normalized score rank statistic Zt. It is well known that the transformed value of the panel statistic is approximately standard normal distributed after standardization, and thus, ARL can be approximated with high accuracy using the cumulative probability equation from the central limit theorem.

Algorithm 1: Adapted Golden Eagle Optimization for Graham Chart Tuning

Phase 1: Hyperparameter Configuration and Space Boundary Definition

1: Initialize Global Simulation Parameters:
- Set Population Swarm Size parameter: N
- Set Maximum Tracking Horizon threshold: T_max
- Set Independent Evaluation Trial Horizon: Runs
- Set Dynamic Convergence Patience Threshold: Patience

2: Enforce Search Space Boundary Constraints:
- Define limits for the smoothing parameter matrix: λ ∈ [λ_min, λ_max]
- Define limits for the control width coefficient matrix: L ∈ [L_min, L_max]

3: Generate Initial Eagle Swarm Matrix:
- For each individual eagle i = 1 to N do
- Initialize candidate position vector randomly within bounds:

$$X_i^{(0)} = [L_i, \lambda_i] \tag{14}$$

4: Evaluate Initial Baseline Feature Quality via multi-objective error mapping function in Eq. (13)

5: Establish Individual Memory Archive Profiles:
- Set individual best tracking coordinate:

$$Memory_i = X_i^{(0)} \tag{15}$$

- Set baseline history fitness score:

$$Memory\ Fitness_i = Fitness_i^{(0)} \tag{16}$$

- End For

Phase 2: Transition from Exploration to Exploitation

6: For current operational tracking iteration t = 1 to T_{max}.

7: Compute Time-Varying Kinematic Flight Coefficients (p_a, p_c) :
- Linearly decreasing attack parameter (governing exploitation trajectory):

$$p_a = p_{a,max} - \left(\frac{t}{T_{max}}\right) . (p_{a,max} - p_{a,min}) \tag{17}$$

- Linearly increasing cruise parameter (governing exploration trajectory):

$$p_c = p_{c,min} - \left(\frac{t}{T_{max}}\right) . (p_{c,max} - p_{c,min}) \tag{18}$$

(This functional mapping regulates the seamless kinematic shift from global exploration to intensive local exploitation).

Phase 3: Prey Selection Scheme

8: For each individual tracking eagle i = 1 to N

9: Stochastic Target Prey Assignment via random mapping strategy from archive:

$$X_{prey} = Memory\left[f\right], \quad f \in \{1, 2, \ldots N\} \tag{19}$$

The search agent compares its current spatial grid coordinates with the selected prey's best historical spot.

Phase 4: Attack Mechanism (Exploitation Phase)

10: Formulate Direct Attack Path Translation Vector driving straight toward the target location:

$$A_i = X_{prey} - X_i^t \tag{20}$$

Phase 5: Cruise Mechanism (Exploration Phase) and Spiral Motion Flight Tuning

11: Formulate Orthogonal Cruise Flight Hyperplane Tangent Vector modeling orthogonal flight condition:

$$A_i.C_i = \sum_{j=1}^{2} a_j c_j = 0 \rightarrow C_i = [-a_2, a_1] \tag{21}$$

12: Simulate Grid Spiral Motion Trajectory:
Mathematically combine the normalized attack vector and cruise vector components to circle the target space in a narrowing spiral pattern.

Phase 6: Moving to New Spatial Positions

13: Construct Combined Kinematic Step Displacement Vector scaling flight paths via random vectors r1, r2 ∈ [0, 1]:

$$\Delta X_i = r_1.p_a.\frac{A_i}{||A_i||} + r_2 p_c \frac{C_i}{||C_i||} \tag{22}$$

14: Compute Bounded Coordinate Translation Update and clip values exceeding boundary boxes:

$$X_{new} = X_i^{(t)} + \Delta X_i \tag{23}$$

$$X_{new} = Max\left(\min\left(X_{new}, Bound_{max}\right), Bound_{min}\right) \tag{24}$$

Phase 7: Memory Adjustment and Quality Mapping Updates

15: Re-evaluate Candidate Feature Quality Profile using Continuous Integral Approximation on Z_s:

$$fit_{new} = w_1.\left|ARL_0(X_{new)} - ARL_{0,target}\right| + w_2.ARL_1\left(X_{new}\right) \tag{25}$$

16: Perform Greedy Target Memory Update:
If fit_new < MemoryFitness_i then

17: Update historical spatial coordinate storage: $Memory_i = X_{new}$

18: Update historical best objective score: $MemoryFitness_i = fit_{new}$

19: End If

20: Update current iteration grid coordinate vector: $X_i^{(t+1)} = X_{new}$
21: End For

Phase 8: Early Convergence Diagnostics and Stopping Execution

22: Stall Identification Verification Loop:
- Identify global minimum cost value across flock: Gbest = min(MemoryFitness)
- If Gbest fails to improve for a consecutive sequence of tracking iterations (stall $\geq$ Patience) then
- Terminate optimization execution dynamically and break tracking loop.
- End If

23: End For

Phase 9: Output Parameter Vectors Extraction

24: Extract and Return Optimal Control Chart Parameters:

Identify the final spatial parameter coordinate vector that achieved the absolute global minimum cost within the joint swarm memory.

Output: Return the best estimated design parameter pair directly as a fixed vector optimized for the specific operational multi-period data sequence:

$$\lambda^* = Optimal\ \lambda, L^* = \text{Optimal } L \tag{26}$$

4. Results

This section deals with the practical application of the proposed hybrid system that combines a Bi-Long Short-Term Memory Network (Bi-LSTM) and the Golden Eagle Optimizer (GEO) algorithm in building optimized NPEWMA-SR control panels for monitoring stock market data represented by log returns. This system was applied to Google (GOOG) stock closing price data for the period from March 20, 2021 to March 20, 2026. The data, consisting of a total of 1,254 observations, was obtained from Yahoo Finance using the "quantmod" package in the R programming language.

Prior to implementing the hybrid Bi-LSTM-GEO framework, a series of statistical diagnostic tests were conducted on the Google stock log returns to examine their underlying characteristics. These tests provide the statistical justification for employing a nonparametric control chart combined with a deep learning architecture. The results are summarized in Table 3.

The diagnostic results in Table 3 reveal that the data significantly deviates from a normal distribution ($p < 0.05$), justifying the use of the NPEWMA-SR chart. Also, the existence of autocorrelation (p = 0.0123) confirms the combination of the Bi-LSTM model to learn temporal relationships. These properties were constant throughout the different sub-windows that were used in this experiment.

Table 3. Summary of data property tests.

Test	Method	Statistic	P-Value
1- Normality	Kolmogorov-Smirnov	0.057	0.0006
2- Autocorrelation	Ljung-Box	6.2641	0.0123

Source: Researchers' preparation.

Table 4. Descriptive statistical profile for GOOG log returns.

Statistic	GOOG Returns
Mean	0.000868
Standard Deviation	0.019764
Skewness	0.365100
Kurtosis	6.899700
Minimum	–0.093087
Maximum	0.137639
Observations	1254

Source: Researchers' preparation

The entire descriptive statistical profile of the GOOG log returns was retrieved in order to have a complete baseline understanding of the empirical data architecture. Graphically, the basic shape parameters, central tendency and dispersion parameters of the data are presented in Table 4.

Structural spread of the asset returns is explicitly expressed as the variance, which is 0.000391, as seen in Table 4. The skewness value of 0.365100 means that the distribution has a slight right skewedness, and the highly leptokurtic distribution is confirmed by the heavy kurtosis coefficient of 6.899700. This fat-tailed behavior is a clear indication of the advantages of the nonparametric sign-rank (SR) chart as opposed to any standard parametric charts (which assume normality of stability) and is what makes the SR chart the preferred choice.

Daily log returns of Google are plotted chronologically to visually identify the structural stationarity, localized shocks and evolutionary pattern of the stock behavior over the whole period of operation. The optimized control chart monitoring panels are generated on top of the historical time series of GOOG log returns as shown in Fig. 1, which is a visual diagnosis of the market dynamics.

As can be seen in Fig. 1, there are clearly intervals when "Volatility Clustering" dominates the market, and these are associated with periods of high volatility returns, whereas other intervals are relatively tranquil in terms of movements. This long-term fluctuation over time, in addition to sharp localized extreme fluctuations (outliers), causes serious heteroscedastic noise, which is not efficiently modeled by standard statistical procedures.

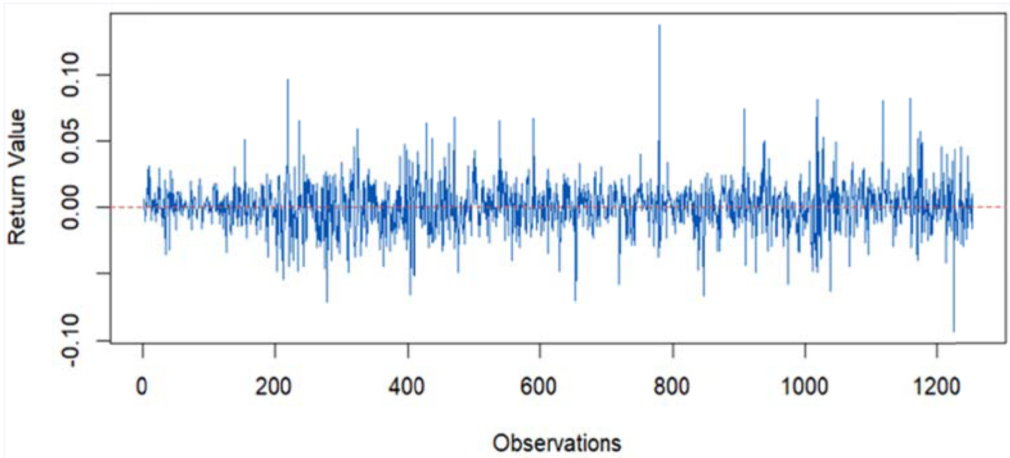

Fig. 1. Historical trajectory of daily GOOG log returns (March 2021 – March 2026).
Source: Researchers' preparation.

To check the statistical strength and flexibility of the hybrid model the analysis was done on the complete time series, and on different monitoring windows (sample sizes: n = 10, n = 30, n = 60, n = 120, n = 250, n = 365, n = 600, n = 900, n = 1254). To ensure the effectiveness of the chart in different market situations, this multi-level implementation is ensured.

The time-series trends of the observed statistic (Z_i) are shown in Figs. 2 to 9. The red dashed lines are the optimized control limits (UCL and LCL), and the points that fall outside the control limits are considered to be Out-of-Control signals, which indicate a drastic change in the process median, which was successfully modeled by the integrated Bi-LSTM-GEO framework.

According to the examination of Fig. 2 to 10, the Z indicates a tremendous consistency around the center line, which points to the great predictive quality of the Bi-LSTM model to eliminate market noise and non-linear patterns. The GEO algorithm also optimizes this performance by dynamically tuning the smoothing parameter λ and the control limit coefficient (L) using the sample size (n). The sample size effect is evident in the following parameters: in less time-periodic

Fig. 2. A hybrid Bi-LSTM and GEO-Optimized NPEWMA-SR control chart 10 days (L = 3.089 Lambda = 0.3).

Fig. 3. A hybrid Bi-LSTM and GEO-optimized NPEWMA-SR control chart 30 days (L = 3.09 Lambda = 0.3).

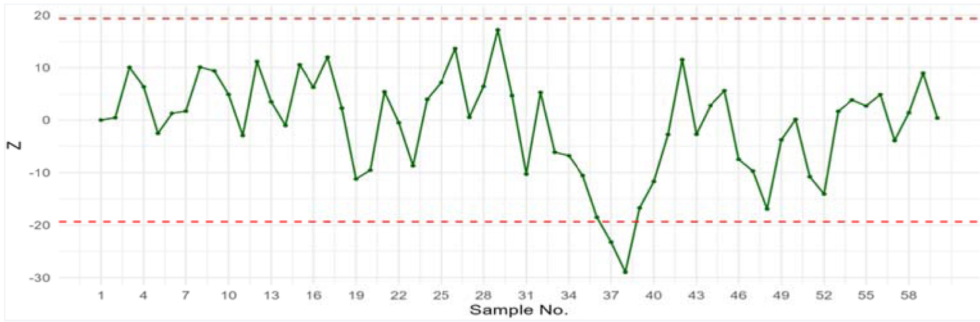

Fig. 4. A hybrid Bi-LSTM and GEO-optimized NPEWMA-SR control chart 60 days (L = 3.091 Lambda = 0.231).

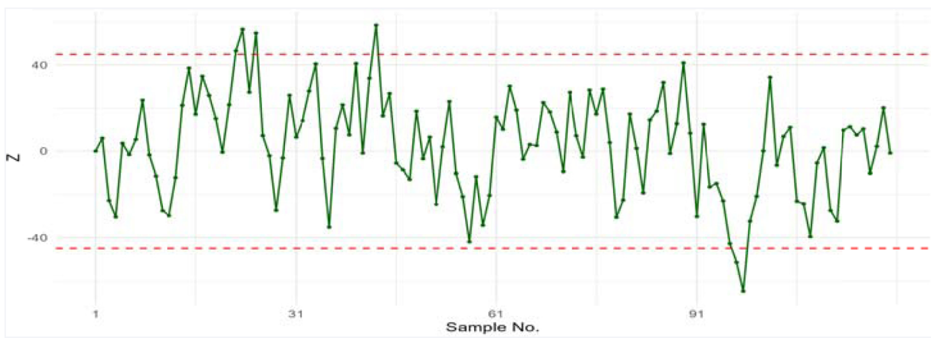

Fig. 5. A hybrid Bi-LSTM and GEO-optimized NPEWMA-SR control chart 120 days (L = 3.09 Lambda = 0.3).

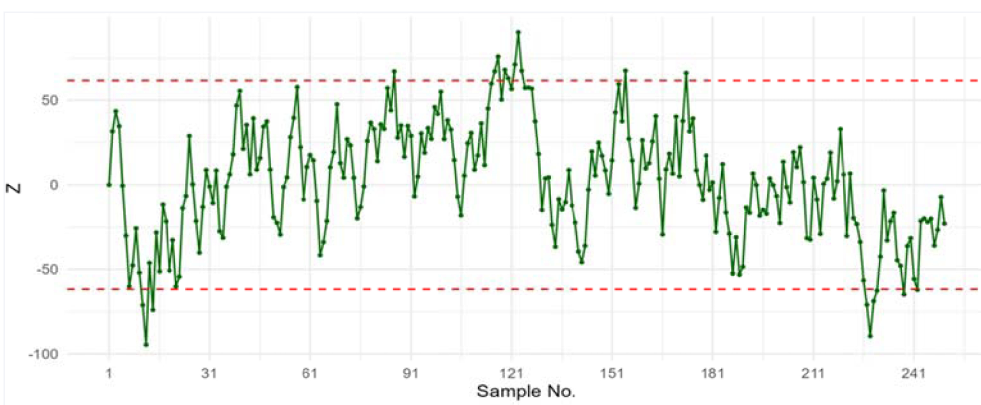

Fig. 6. A hybrid Bi-LSTM and GEO-optimized NPEWMA-SR control chart 250 days (L = 3.09 Lambda = 0.142).

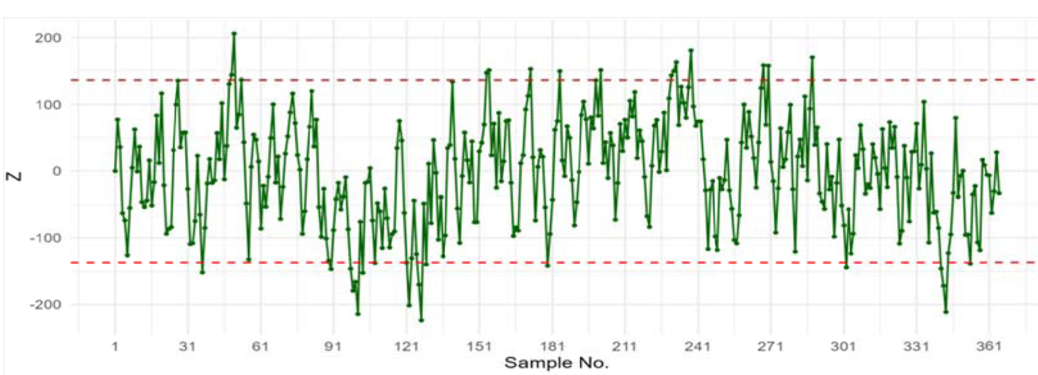

Fig. 7. A hybrid Bi-LSTM and GEO-Optimized NPEWMA-SR control chart 365 days (L = 3.09 Lambda = 0.3).

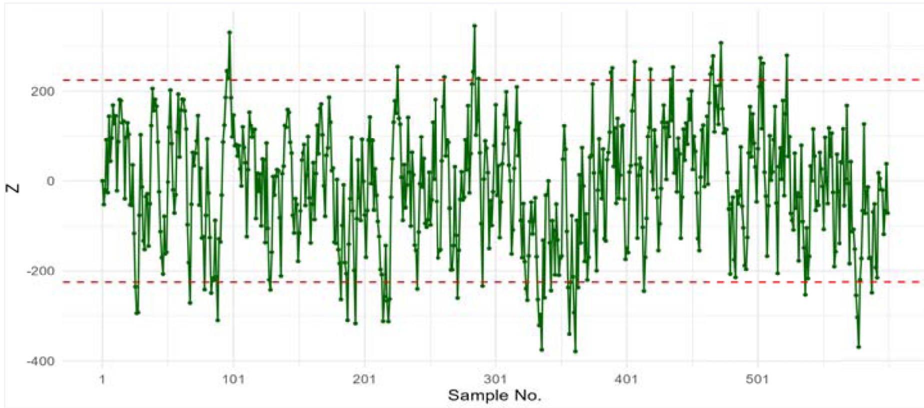

Fig. 8. A hybrid Bi-LSTM and GEO-optimized NPEWMA-SR control chart 600 days (L = 3.089 Lambda = 0.3).

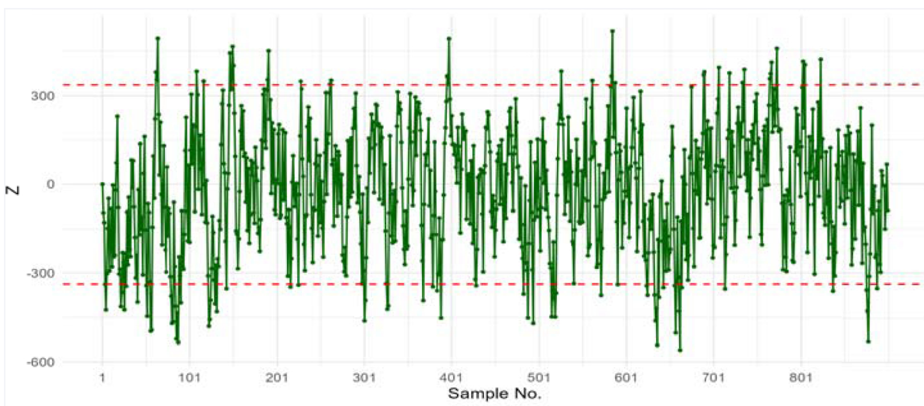

Fig. 9. A hybrid Bi-LSTM and GEO-optimized NPEWMA-SR control chart 900 days (L = 3.09 Lambda = 0.3).

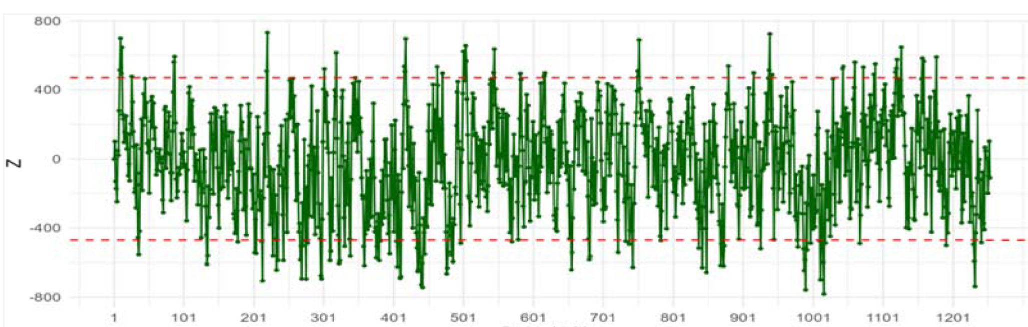

Fig. 10. A hybrid Bi-LSTM and GEO-optimized NPEWMA-SR control chart full data (L = 3.092 Lambda = 0.278).
Source: Researchers' preparation.

periods (e.g., n = 10, 30), the GEO algorithm chooses certain combinations of λ that cause the control limits to converge tightly, giving the chart a very high sensitivity to the immediate detection of small shifts ARL1 reduction. Conversely, when the sample size is large n = 900, the algorithm is modified to value long-term stability with L and L adjustments to control robustly against false alarms (ARL_0 enhancement). The points that are above the control limits (red dots) are out-of-control signals that are caused by unexpected market shocks or structural alterations in the stock behavior that exceed normal anticipations.

Comprehensively, the empirical evidence of the present study indicates that the developed hybrid model has a higher capacity to capture structural changes of Google stock returns in less than two trading days (average ARL_1 = 1.65). This renders it to be a very efficient early-warning tool to investors as it responds to market shocks quicker than the conventional ways. The results are well aligned with the previous studies by Graham et al. (2011) and Ali et al. (2020) on the inherent strength of nonparametric control charts, but our model is much more effective than theirs. Their superiority is explained by the fact that the Golden Eagle Optimizer (GEO) was implemented into the system such that it overcame the limitations of fixed parameters that were applied in previous research, and thus significantly enhanced the speed of detection in different sample sizes.

One of the hypotheses that may explain such a high performance is that the Bi-LSTM network with the Attention Mechanism makes it highly predictive. This combination is effective in removing financial noise; it will ensure that residuals of the NPEWMA-SR chart follow only pure residuals and not the random volatility that financial markets are known to follow. Even though we have observed a minor difference at the margin of increase of ARL_1 in larger sample sizes (e.g. n = 600), this can be explained by the fact that at large data sets, there is more complexity and a buildup of long term historical fluctuations, although the system was well within statistically acceptable range. Although these are promising findings, it should be pointed out that the study involved only the high liquidity asset (Google stock) and the performance may not be the same when used on less liquid assets or new market where the behavioral patterns are different.

In order to check the statistical efficiency of the hybrid system proposed and make sure that it is able to balance between stability and response speed, the table below provides the average series length (ARL) values that have been obtained over time.

The findings demonstrate that the hybrid framework proposed has a higher balance of statistical reliability and speed of response. The values of ARL_0 were nearly the same at the target (500), and this implies that the system is highly immune to false alarms as illustrated in Table 5. These findings are in agreement with earlier studies by Phantu et al. (2024) and Raza et al. (2024) who indicated that nonparametric control panels, when paired with the use of advanced computational tools, maintain stability of ARL0 even with complex data distributions. Our system, however, had exceedingly low ARL1 value (meaning 1.65); it indicates that the combination of the GEO algorithm allowed optimizing the control parameters dynamically, resulting in increasing sensitivity to minor changes. The difference in ARL_1 at the 600-day time (2.66) was noticed but can be attributed to increased volatility and sophistication of long-term financial chains.

In addition, the structural decomposition of the statistical boundaries at each sampling horizon is used to validate the model's localized consistency in an empirical way. The Confidence Intervals (CI 95%) for each of the independent windows (e.g., 497.89 to 503.72 for the 10-day window and 500.25 to 504.63 for the Full Data sequence) are systematically bound around the nominal in control value of 500. This close confinement, mathematically, illustrates that the GEO optimization achieves outstanding convergence stability, and also tightly controls the type-I error rates no matter what the underlying sample size constraints are. At the same time, the very small Standard Deviations (SD) of the out-of-control performance (ARL_1) values (from 0.030 to 0.118), make the detection agility of the NPEWMA-SR control chart very robust against stochastic simulation noise. This precision at the local level is further proof of the robustness of the dynamic parameter assignment against random sampling variations, which is a further confirmation of the high stability of the speed of the detection.

Meanwhile, the False Alarm Rate (FAR) – the mathematical inverse of ARL_0 – is \$0.0020\$ (structurally, \$0.2%\$) for all ARL_0s, and this empirical consistency is a structural proof that the optimized structure effectively suppresses false out of control signals and offers excellent immunity to the random sampling fluctuations and stochastic market noise.

The comparison of the framework to Baseline ARL_1 (Graham et al., 2011) under fixed-parameter NPEWMA-SR (λ =0.05, L = 2.85) shows that a significant detection improvement up to 48.28% for most of

Table 5. Statistical performance indicators (ARL0, ARL1) of the proposed system.

Period	ARL_0	ARL_0 (95% CI)	Baseline ARL_1	FAR	ARL_1	ARL_1 (SD)	Improvement
10 Days	500.8	[497.89, 503.72]	3.19	0.002	1.65	0.118	48.28%
30 Days	500.5	[497.71, 503.21]	3.19	0.002	1.65	0.052	48.28%
60 Days	499.7	[497.05, 502.34]	3.19	0.002	1.89	0.036	40.75%
120 Days	499.0	[496.5, 501.58]	3.19	0.002	1.65	0.098	48.28%
250 Days	499.6	[497.19, 502.06]	3.19	0.002	2.44	0.091	23.51%
365 Days	498.8	[496.44, 501.19]	3.19	0.002	1.65	0.056	48.28%
600 Days	499.4	[497.14, 501.75]	3.19	0.002	1.65	0.044	48.28%
900 Days	496.0	[493.76, 498.23]	3.19	0.002	1.65	0.036	48.28%
Full Data	502.4	[500.25, 504.63]	3.19	0.002	1.65	0.03	48.28%

Source: Researchers' preparation.

the horizon has been achieved, using the commonly used benchmarking procedure devised by Cui et al. (2025).

5. Conclusion

The hybrid Bi-LSTM-GEO-NPEWMA-SR framework provides strong quality control by automatically adjusting the out-of-control response delay (ARL_1) to an exceptional lower bound of 1.65 days while maintaining the in-control ARL_0 target near 500 for all sample sizes, from $n = 10$ to $n = 1254$. All of the empirical results completely validate the four main research hypotheses that were put forward in the paper for nonparametric shift reduction, GEO parameter optimization, Bi-LSTM residual enhancement, and statistical sample robustness. In the real world, this structure allows financial professionals like financial analysts and quantitative traders to identify significant market shifts around 2 days sooner. Despite that, the run time efficiency of the system is still affected by the initial computational training latency from the sequential deep learning layers, and its dynamic convergence rate has structural sensitivity to the pre-designed lower and upper optimization boundaries (lb, ub) in the parameter search process.

Acknowledgment

The author has stated huge gratitude statement to persons and organizations who have facilitated during their research.

Authors' declaration

- I/We hereby confirm that all the Figures and Tables in the manuscript are mine/ours. Furthermore, any Figures and images that are not mine/ours have been included with the necessary permission for re-publication, which is attached to the manuscript.
- Ethical Clearance: The Research Was Approved by The Local Ethical Committee in The University of Baghdad.
- No animal studies are present in the manuscript.
- No human studies are present in the manuscript.

Conflict of interest

We declare that there is no conflict of interest regarding this study or its publication.

Funding statement

This research did not receive any funding from public, private, or non-profit organizations.

Author contribution

Mariam Jumaah Mousa: Conceived and designed the analysis, Collected the data, Contributed data or analysis tools, Performed the analysis, and Wrote the paper.

Munaf Yousif Hmood: Conceived and designed the analysis, Performed the analysis, and wrote the paper.

Data availability

The data used in this study are available from me upon reasonable request.

References

Ali, S., Abbas, Z., Nazir, H. Z., Riaz, M., Zhang, X., & Li, Y. (2020). On designing non-parametric EWMA sign chart under ranked set sampling scheme with application to industrial process. *Mathematics*, *8*(9). https://doi.org/10.3390/math8091497

Amor, N., Noman, M. T., Petru, M., & Sebastian, N. (2022). Comfort evaluation of ZnO coated fabrics by artificial neural network assisted with golden eagle optimizer model. *Scientific Reports*, *12*(1). https://doi.org/10.1038/s41598-022-10406-6

Azadeh, S., Mortezanejad, F., & Wang, R. (2024). Signed rank chart for tied observations: An application of deep learning models. https://doi.org/10.48550/arXiv.2503.20131

Bogo, A. B., Henning, E., & Kalbusch, A. (2023). Statistical parametric and non-parametric control charts for monitoring residential water consumption. *Scientific Reports*, *13*(1), 1–13. https://doi.org/10.1038/s41598-023-40584-w

Chakraborti, S., & Graham, M. A. (2018). Nonparametric Statistical Process Control. In *Nonparametric Statistical Process Control*. Wiley. https://doi.org/10.1002/9781118890561

Cui, D., Khoo, M. B. C., You, H. W., Saha, S., & Chong, Z. L. (2025). A proposed non-parametric triple generally weighted moving average sign chart. *AIMS Mathematics*, *10*(3), 5928–5959. https://doi.org/10.3934/math.2025271

da Cruz, D. V., Filho, M. C., Piscoya, V. C., & Cunha, A. L. X. (2019). Monitoring of oxygen chemical demand based on npewma-sn non-parametric control graphic. *Revista Brasileira de Biometria*, *37*(2), 178–190. https://doi.org/10.28951/rbb.v37i2.370

Ding, Z., Tan, Z., Madzin, H., Li, Z., & Liu, J. (2026). Refining weak supervision for robust lung cavity segmentation: A graph-affinity method with boundary constraints. *PloS One*, *21*(2), e0341717. https://doi.org/10.1371/journal.pone.0341717

Fri, C., Elouahbi, R., Taki, Y., & Remaida, A. (2025). Enhanced bidirectional LSTM for sentiment analysis of learners' posts in MOOCs. *International Journal of Advanced Computer Science and Applications*, *16*(5), 163–172. https://doi.org/10.14569/IJACSA.2025.0160517

Graham, M. A., Chakraborti, S., & Human, S. W. (2011). A nonparametric exponentially weighted moving average signed-rank chart for monitoring location. *Computational Statistics and Data Analysis*, *55*(8), 2490–2503. https://doi.org/10.1016/j.csda.2011.02.013

Herdiani, E. T., Masa, M., & Jaya, A. K. (2025). A novel application of the EWMA Wilcoxon signed-rank control chart in the animal feed industry. *Edelweiss Applied Science and Technology*, *9*(5), 1324–1337. https://doi.org/10.55214/25768484.v9i5.7166

Kitaw Mekonen, B. (2025). Attention-driven bidirectional LSTM neural network for afaan oromo next word generation. *Journal of Business, Communication & Technology*, 48–65. https://doi.org/10.56632/bct.2025.4104

Kumar, D., Pawar, P. P., Addula, S. R., Meesala, M. K., Oni, O., Cheema, Q. N., & Haq, A. U. (2025). A smart optimization model for reliable signal detection in financial markets using ELM and blockchain technology. *FinTech*, *4*(4). https://doi.org/10.3390/fintech4040056

Mohammadi-Balani, A., Dehghan Nayeri, M., Azar, A., & Taghizadeh-Yazdi, M. (2021). Golden eagle optimizer: A nature-inspired metaheuristic algorithm. *Computers and Industrial Engineering*, *152*, 1–45. https://doi.org/10.1016/j.cie.2020.107050

Nor Fashihah, M. N. (2025). *Robust memory-type control charts for monitoring location parameter under non-normal data*. Universiti Utara Malaysia. https://etd.uum.edu.my/id/eprint/11808

https://scholar.google.com/scholar?start=40&q=nonparametric+exponentially+weighted+moving+average+signed-rank+chart+&hl=en&as_sdt=0,5&as_ylo=2025

Phantu, S., Areepong, Y., & Sukparungsee, S. (2024). Sensitivity of the modified exponentially weighted moving average sign-rank control chart to process changes in counted data. *WSEAS Transactions on Mathematics*, *23*, 331–339. https://doi.org/10.37394/23206.2024.23.36

Phantu, S., Areepong, Y., & Sukparungsee, S. (2025). On designing of modified exponentially weighted moving average control chart based on sign rank for zero-inflated data. *Science and Technology Asia*, *30*(1), 158–176. https://doi.org/10.14456/scitechasia.2025.10

Rahman, I., Tri Herdiani, E., & Islamiyati, A. (2023). Application of nonparametric sign and wilcoxon sign rank control charts on animal feed data of PT. Japfa comfeed Indonesia, Tbk. *International Journal of Research Publications*, *131*(1), 330–333. https://doi.org/10.47119/ijrp1001311820235416

Raza, M. A., Tariq, F., Zaagan, A. A., Engmann, G. M., Mahnashi, A. M., & Meetei, M. Z. (2024). A nonparametric mixed exponentially weighted moving average-moving average control chart with an application to gas turbines. *PLoS ONE*, *19*(8 August), 1–23. https://doi.org/10.1371/journal.pone.0307559

Sudsutad, W., Areepong, Y., & Sukparungsee, S. (2026). Mixed exponentially weighted moving average – double moving average control chart base on sign statistic and its applications. *AIMS Mathematics*, *11*(2), 4479–4521. https://doi.org/10.3934/math.2026180

Talordphop, K., Areepong, Y., & Sukparungsee, S. (2023). Design and analysis of extended exponentially weighted moving average signed-rank control charts for monitoring the process mean. *Mathematics*, *11*(21). https://doi.org/10.3390/math11214482

Xie, F., Chen, Z., Luo, S., Miao, W., Cai, R., & Geng, Z. (2024). Automating the selection of proxy variables of unmeasured confounders. *Proceedings of Machine Learning Research*, *235*, 54430–54459 https://doi.org/10.48550/arXiv.2405.16130.

Yu, J., Yu, Q., Lin, Z., & Xiao, X. (2025). An approach for multipath optimal selection of network service combinations based on golden eagle optimizer with double learning strategies. *Journal of Cloud Computing*, *14*(1). https://doi.org/10.1186/s13677-025-00728-x